Catalysis Today 316 (2018) 114–121

Contents lists available at ScienceDirect

Catalysis Today

journal homepage: www.elsevier.com/locate/cattod

Effect of mass-transfer control on HY zeolites for dimethoxymethane carbonylation to methyl methoxyacetate

Dongxi Zhang[b], Lei Shi[a,b,*], Yan Wang[b], Fei Chen[b], Jie Yao[b], Xinyu Li[b], Youming Ni[a], Wenliang Zhu[a], Zhongmin Liu[a,*]

[a] National Engineering Laboratory for Methanol to Olefins, Dalian National Laboratory for Clean Energy, Dalian Institute of Chemical Physics, Chinese Academy of Sciences, Dalian, 116023, PR China
[b] Institute of Industrial Chemistry and Energy Technology, Shenyang University of Chemical Technology, Shenyang, 110142, PR China

ARTICLE INFO

Keywords:
Mass-transfer control
Carbonylation
Mesopore
DMM
MMAc
HY zeolite

ABSTRACT

A series of hierarchical HY zeolites were prepared by using sequential acid (H_4EDTA) and alkaline (NaOH and NH_4OH) solution treatments. The nitrogen adsorption-desorption analysis proved that the mesoporous structure was definitely formed with the pore diameter at about 3.5 and 17.5 nm, and the external surface area and mesopore volume significantly increased. The XRD, XRF, and NH_3-TPD characterization results disclosed that the relative crystallinity, crystalline sizes, and acidity of as-treated HY zeolites decreased as compared with parent HY although their Si/Al ratios were higher. The zeolites were conducted in vapor phase carbonylation of dimethoxymethane (DMM) to methoxyacetate (MMAc) at 5.0 MPa and different temperatures. As compared with reference HY, the DMM conversion and MMAc selectivity obviously increased from 50.41% to 90.91% and from 34.79% to 84.57% at 383 K, respectively. The DMM conversion were closely related to the medium-strong acid amount and greater amount of medium-strong acid sites resulted in higher DMM conversion. The catalytic stability of HY-$DAl_{0.11}$-$DSi_{NaOH0.05}$ was carried out at 393 K and 5.0 MPa for 100 h. The DMM conversion (about 97%) and products selectivity (MMAc: 84%) kept unchanged during the whole carbonylation process, exhibiting excellent catalytic stability, which was also supported by the TG-DTA analysis that the carbon deposition was effectively suppressed. In a word, as-treated HY zeolites with larger external surface area and mesopore volume that contributed to promoting the mass transfer efficiency exhibited much higher DMM conversion, MMAc selectivity and excellent catalytic stability than parent HY.

1. Introduction

Over the past decade, hierarchical zeolites, which have unique pore sizes [1] with micro/mesoporous structure [2,3], received much attention because of its enhanced performance in some catalytic reactions with space and diffusion limitations problems [4]. For example, the conversion and selectivity of benzene alkylation are obviously promoted with hierarchical catalysts instead of micropore zeolites because of enhanced accessibility [5] and diffusion [6,7]. Hierarchical zeolites used in Fischer-Tropsch synthesis can obviously improve the mass transport and increase the selectivities of C_5–C_{11} hydrocarbons [8]. Besides, the catalytic stability of hierarchical HZSM-5 for methanol to gasoline reaction [9] is significantly improved.

Methyl methoxyacetate (MMAc) is a kind of high value-added and important fine chemical. Recently, MMAc is mainly used in manufacture of protectants and pharmaceuticals [10]. Nevertheless, only a few literatures or patents reported the synthesis routes of MMAc, as below: reaction of methyl chloroacetate with sodium methoxide [11], couple of formaldehyde derivatives with methyl formate [12,13], and carbonylation of dimethoxymethane (DMM) [14,15].

In former work [15], the DMM conversion reached about 100% with high MMAc selectivity (74.32%) via the D-009B catalyst and sulfolane as a solvent under 383 K and 5 MPa for 6 h. D-009B, a kind of sulfonic acid resin catalyst, has strong acidity and is beneficial for DMM carbonylation to produce MMAc. However, the sulfonic acid group in the as-used catalyst was continuously taken off by the reactants and products in a long-time reaction process. A.T. Bell reported the vapor phase cabonylation of DMM to MMAc with 79% selectivity by using H-FAU zeolite [14]. After that, lots of efforts had been made in studying the effect of different topological structures and Si/Al ratios of zeolites on DMM carbonylation. FAU had a very high selectivity to MMAc as compared with MFI, MOR and BEA [16–18]. It was proposed [16,17]

* Corresponding authors at: National Engineering Laboratory for Methanol to Olefins, Dalian National Laboratory for Clean Energy, Dalian Institute of Chemical Physics, Chinese Academy of Sciences, Dalian, 116023, PR China. Institute of Industrial Chemistry and Energy Technology, Shenyang University of Chemical Technology, Shenyang, 110142, PR China.
E-mail addresses: shilei1982@dicp.ac.cn (L. Shi), liuzm@dicp.ac.cn (Z. Liu).

https://doi.org/10.1016/j.cattod.2018.02.004
Received 3 December 2017; Received in revised form 26 January 2018; Accepted 2 February 2018
Available online 08 February 2018
0920-5861/

that the low rate of MMAc formation observed at low Si/Al ratios was due to the repulsive interactions between adsorbed species located within the same supercage or channel intersection.

We consider that the diffusion and mass transfer efficiency of MMAc is limited in FAU micropore channels due to its small pore opening (0.74 nm) and large molecular weight (104.1 g/mol). More importantly, a low mass transfer rate of MMAc could result in the deactivation of as-used zeolites because the heavy products remaining on the acid centers in the channel are beneficial for the formation of carbon deposition, that readily covers the active sites. Hence, the hierarchical FAU with large external surface area and mesoporous will significantly contribute to the mass transfer efficiency of MMAc, leading to the increase of MMAc selectivity and catalytic stability.

Currently, bottom-up [19–21] and top-down [22–25] methods are usually applied to synthesize hierarchically structured zeolites. For bottom-up approaches, the mesopore introduced with the usage of templates and the microporous are one-step synthesized [26,27] simultaneously. However, bottom-up methods are difficult for industrial manufacture because mesopore-inducing agents are highly expensive and non-readily available [27]. For top-down methods, the micropore zeolites are used as starting materials and the mesoporous are introduced by post-synthetic treatments [28]. In fact, post-synthetic treatments like desilication [28–31] and dealumination [31–33] processes are easily-operated and economical.

In this paper, HY with Si/Al = 2.70 was applied as the reference and initial precursor. The hierarchical HY zeolites were pretreated by using sequential acid (H_4EDTA) and alkaline (NaOH and NH_4OH) solution treatments. The dealumination process should be carried out before desilication because the framework Si is difficult to be removed to form a hierarchical structure in high Al content of the zeolites [28,34]. Although the acid amount, acid strength, and crystallinity of the as-treated hierarchical HY zeolite decreased, the DMM conversion, MMAc selectivity, and catalytic stability were significantly enhanced because of its larger external surface area, mesopore structure, and the promoted mass transfer ability.

2. Experimental section

2.1. Catalyst preparation

HY zeolite (Nankai University Catalyst Co, bulk Si/Al = 2.70, H-form as a reference). **Dealumination:** HY (13.40 g) was first added into 200 mL H_4EDTA solution and stirred at 338 K for 6 h, followed by filtration and washing with deionized water for three times. The desired sample was dried at 393 K for 8 h, followed by calcination at 823 K for another 4 h in air to obtain the precursor, noted as HY-DAl_n. **Desilication:** HY-DAl_n (1.70 g) was poured into 50 mL NaOH or NH_4OH solution and stirred at 338 K or at room temperature for 30 min, followed by filtration and washing with deionized water for three times. The desired sample was dried at 393 K for 8 h, followed by calcination at 823 K for another 4 h in air to obtain the precursor. Alkaline treatment using NaOH treatments was labeled as "DSi_{NaOHn}", and NH_4OH treatments was noted as "DSi_{NH4OHn}" (DSi: desilication). In all cases, the suffix "*n*" represents the concentration of the solution. After dealumination and desilication pretreatments, 10 g precursor was converted into its NH_4^+ form by exchanging with 100 mL NH_4NO_3 (1 mol/L) aqueous solution at 338 K for 2 h, followed by filtration and washing with deionized water. The desired sample was dried at 393 K for 8 h, followed by calcination at 823 K for another 6 h in air to obtain HY-DAl_n-DSi_n.

2.2. Catalyst characterization

Powder X-ray diffraction (XRD) patterns were acquired with a Bruker D8 advance diffractometer using Cu K α (λ = 0.15406 nm) radiation. Data was recorded in the 2 θ range from 5 to 45° with a step size of 0.05° at 40 kV and 40 mA. The HY zeolite crystallite average size as calculated by the Scherrer formula. Besides, the variation in zeolite crystallinity resulting from post-synthetic modifications was derived from the relative intensity of the reflection (533) at 2θ of 23.58°, assuming that the reference crystallinity is 100% [28].

A Bruker S4 pioneer advanced X-ray fluorescence (XRF) spectrometer was used to determine the chemical composition with different Si/Al ratios.

N_2 isotherms were measured in a Quantachrome (Autosorb iQ Statio) instrument at 77 K after the treatment of samples at 573 K in vacuum for 3 h. The surface area was determined by using a Brunauer-Emmett-Teller (BET) method. Barrett-Joyner-Halenda (BJH) and Horváth-Kawazoe (HK) methods were applied to calculate the pore size distribution in the mesopore and micropore region, respectively.

The NH_3-TPD experiments were carried out on a Builder PCA-1200. The sample (ca. 200 mg) was pretreated at 573 K in a flow of 30 mL/min He for 1 h. After the pretreatment, the sample was cooled to 353 K and exposed to NH_3 for 10 min. Then, the physically adsorbed NH_3 should be removed by He at the same temperature until the baseline was stable. Thereafter, NH_3-TPD was conducted in a constant flow of He (30 mL/min) from 373 to 973 K at a heating rate of 10 K/min. The amount of desorbed NH_3 was detected by a thermal conductivity detector.

TG-DTA analysis proceeded in the thermal analysis equipment (STA 449C Jupiter, NETZSCH). 2 mg precursor was performed in a flow of 80 mL/min air with the temperature increasing from 313 to 1073 K at a heating rate of 10 K/min.

2.3. Catalytic reaction

The vapor phase carbonylation of dimethoxymethane (DMM) was performed using 1 g catalyst at 5.0 MPa CO in a continuous flow fixed-bed stainless steel reactor with an 8.5 mm inner diameter. 20 mL/min CO bubbled through a stainless-steel saturator filled with DMM (98%, Aladdin) maintained at room temperature and 80 mL/min pure CO were mixed together and introduced into the reactor. All the reaction products were analyzed online by a gas chromatograph (GC-2014C) equipped with a HP-FFAP capillary column connected to a flame ionization detector. The conversion of DMM and the products selectivities were calculated on the basis of weight, as follows [17]: DMM Conv. = $(DMM_{in} - DMM_{left})/DMM_{in}$; MMAc selectivity was calculated on the basis of weight, MMAc Sel. = $MMAc_{formation}$/the mass of all products.

3. Results and discussion

3.1. XRD and XRF analysis of the as-treated hierarchical HY zeolites

The X-ray diffraction (XRD) patterns of HY, HY-$DAl_{0.11}$ (pretreated by 0.11 M H_4EDTA solution for dealumination), HY-$DAl_{0.15}$ (by 0.15 M H_4EDTA) and HY-$DAl_{0.15}$-$DSi_{NH4OH0.05}$ (by 0.15 M H_4EDTA and further pretreated by 0.05 M NH_4OH for desilication) are displayed in Fig. 1(A). The crystalline sizes of HY, HY-$DAl_{0.11}$, HY-$DAl_{0.15}$, and HY-$DAl_{0.15}$-$DSi_{NH4OH0.05}$, which were derived from the strongest intensity of the reflection (331) at 2θ of 16.25° and calculated by the Scherrer formula, were 36.60, 33.50, 29.20, and 20.20 nm, respectively. The crystallinity of as-treated HY catalysts calculated by comparing the relative intensity divided by the reference at 2θ of 23.58° were 58.39%, 22.93%, and 18.68%, assuming that the crystallinity of reference HY was 100%. Above mentioned results evidently demonstrated that with increasing the concentration of H_4EDTA, the relative crystallinity gradually decreased and the crystalline sizes also slowly reduced. After dealumination by H_4EDTA solution, further desilication by NH_4OH resulted in much more serious collapse of crystal structure. As known, H_4EDTA was a kind of chelating agent that could remove the Al atoms from the framework of zeolite [28]. Therefore, more Al atoms were extracted

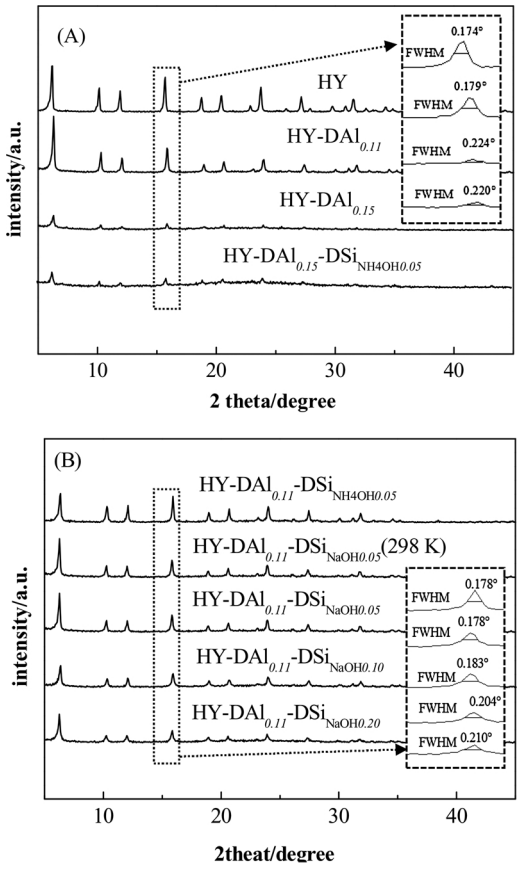

Fig. 1. XRD analysis of the as-treated hierarchical HY zeolites.

from HY with the increased amount of H_4EDTA under the same conditions, leading to the generation of more vacancies and even the partial amorphization of framework. Meanwhile, the expelling of Al resulted in the formation of intergranular and intercrystalline pores.

The XRD patterns of HY-DAl$_{0.11}$-DSi$_{NH4OH0.05}$ (further pretreated by 0.05 M NH_4OH for desilication based on HY-DAl$_{0.11}$), HY-DAl$_{0.11}$-DSi$_{NaOH0.05}$ (298 K) (by 0.05 M NaOH but at 298 K), HY-DAl$_{0.11}$-DSi$_{NaOH0.05}$ (by 0.05 M NaOH), HY-DAl$_{0.11}$-DSi$_{NaOH0.10}$ (by 0.10 M NaOH), and HY-DAl$_{0.11}$-DSi$_{NaOH0.20}$ (by 0.20 M NaOH) are exhibited in Fig. 1(B). The relative crystallinity of as-treated catalysts was 62.84%, 55.20%, 48.62%, 40.98%, and 35.67%, as well as the crystalline size was 35.10, 34.40, 34.00, 32.80, and 32.60 nm, respectively. These results indicated that both relative crystallinity and crystalline sizes gradually decreased with increasing the concentration of NaOH, especially under the heating condition. OH^- could break the Si−O−Si and Si−O−Al bonds to produce soluble silicate, aluminate, and aluminosilicate species which could leave from the surface of the dissolving HY, resulting in the formation of vacancies [35] and generation of intracrystalline mesoporous [26]. Under the heating condition, Si atoms were more readily removed from the framework of HY [36]. Higher NaOH concentration also contributed to the expelling of Si but easily led to the partial framework amorphization [37]. The crystallinity and crystalline size of HY-DAl$_{0.11}$-DSi$_{NH4OH0.05}$ were lower than those of HY-DAl$_{0.11}$-DSi$_{NaOH0.05}$ (298 K). These phenomena could be explained by the fact that the alkalinity of NaOH was stronger than that of NH_4OH. NaOH was completely ionized to Na^+ and OH^- in solution. While upon contacting HY with NH_4OH solution, Si was extracted from the zeolite framework by OH^- in mediated hydrolysis [30,38] condition. Hence, the desilication effect of NaOH was stronger than that of NH_4OH although the precursor was treated at lower temperature.

The Si/Al ratios of as-prepared catalysts were measured by X-ray fluorescence (XRF) and the results are listed in Table 1. The Si/Al ratio of HY, HY-DAl$_{0.11}$, and HY-DAl$_{0.15}$ was 2.70, 5.49, and 6.03, suggesting that the Si/Al ratio increased with the increased H_4EDTA concentration. The Si/Al ratio of HY-DAl$_{0.11}$-DSi$_{NaOH0.05}$, HY-DAl$_{0.11}$-DSi$_{NaOH0.10}$, HY-DAl$_{0.11}$-DSi$_{NaOH0.20}$, and HY-DAl$_{0.11}$-DSi$_{NaOH0.05}$ (298 K) were 4.08, 3.25, 2.84, and 4.68, illustrating that with the increased NaOH solution concentration, the Si/Al ratio gradually decreased and more Si atoms were extracted under the heating condition. The Si/Al ratio of HY-DAl$_{0.11}$-DSi$_{NH4OH0.05}$ and HY-DAl$_{0.15}$-DSi$_{NH4OH0.05}$, which had an inverse relationship after desilication under the same condition, were 4.80 and 3.96, while the initial Si/Al ratio of HY-DAl$_{0.11}$ and HY-DAl$_{0.15}$ were 5.49 and 6.03, proving that Si in the framework of HY with low Al content was more easily extracted. This phenomenon was in good accordance with the report [26] that the framework Si was difficult to be removed in high Al content of zeolites because the negatively charged AlO_4^- would prevent OH^- from further extracting Si.

3.2. Nitrogen adsorption-desorption analysis

The adsorption-desorption isotherms of HY, HY-DAl$_{0.11}$, HY-DAl$_{0.15}$, HY-DAl$_{0.15}$-DSi$_{NH4OH0.05}$, HY-DAl$_{0.11}$-DSi$_{NH4OH0.05}$, HY-DAl$_{0.11}$-DSi$_{NaOH0.05}$ (298 K), HY-DAl$_{0.11}$-DSi$_{NaOH0.05}$, and HY-DAl$_{0.11}$-DSi$_{NaOH0.10}$ are shown in Fig. 2. All the pretreated catalysts exhibited a type-IV isotherm containing a hysteresis loop at a relative pressure higher than $P/P_0 = 0.4$ value, that evidently indicated the existence of mesopore structure [1]. The hysteresis loop of as-treated zeolites was much larger than that of the parent HY, suggesting that their pore sizes were larger than that of the reference HY [39]. The hysteresis loop of HY-DAl$_{0.15}$ was significantly smaller than those of the other treated zeolites, indicating that the pore size of HY-DAl$_{0.15}$ decreased after treatment by 0.15 M H_4EDTA solution for dealumination. We recognized that higher H_4EDTA concentration resulted in partial amorphization of the zeolite structure and the pore was clogged with amorphous aluminosilicate debris [28,40]. This phenomenon was in good accordance with XRD analysis and proved in the subsequent pore sizes distribution.

The pore sizes distribution of different samples in micropore region calculated by a HK method from 0.3 to 2 nm and in mesoporous region determined by a BJH method from 2 to 50 nm the are exhibited in Fig. 3(A) and (B), respectively. All the samples displayed a unimodal pore in micropore region. The micropore size and intensity of HY were 0.56 nm and 1.56 $cm^3\,g^{-1}\,nm^{-1}$, respectively. After dealumination by 0.11 M H_4EDTA solution, the micropore size decreased to 0.50 nm, but the peak intensity increased to 2.53 $cm^3\,g^{-1}\,nm^{-1}$, much larger than that of HY, suggesting that the micropore amount obviously increased. With the H_4EDTA concentration increasing to 0.15 M, the micropore size slightly decreased to 0.49 nm, but the peak intensity significantly decreased to 0.57 $cm^3\,g^{-1}\,nm^{-1}$, indicating that the micropore amount obviously reduced. When HY-DAl$_{0.15}$ was further treated with 0.05 M NH_4OH, the micropore size slightly increased to 0.54 nm, while the micropore intensity decreased to 0.45 $cm^3\,g^{-1}\,nm^{-1}$. When HY-DAl$_{0.11}$ was further treated with different bases in the order of 0.05 M NH_4OH (298 K), 0.05 M NaOH (298 K), 0.05 M NaOH (338 K), and 0.10 M NaOH (338 K), the micropore size (centered at about 0.58 nm) nearly kept unchanged, nevertheless the micropore intensity continuously decreased from 1.56 to 1.25, 1.15, 1.02, and 0.84 $cm^3\,g^{-1}\,nm^{-1}$, demonstrating that the micropore amount gradually decreased with the increased basic strength, treating temperature, and alkali content. For the parent HY zeolite, two peaks centered at around 3.41 and 17.51 nm in mesoporous region were attributed to the small and large mesoporous, and the counterpart intensity were 0.10 and 0.09 $cm^3\,g^{-1}\,nm^{-1}$, respectively. After dealumination by 0.11 M H_4EDTA solution, the small mesopore size nearly remained the same and the intensity slightly decreased to 0.09 $cm^3\,g^{-1}\,nm^{-1}$; the large mesopore size increased to 18.32 nm and the intensity rose to 0.10 $cm^3\,g^{-1}\,nm^{-1}$. With the H_4EDTA concentration increasing to 0.15 M, the peak of small mesoporous disappeared and the only large

Table 1
Characterization of different catalysts.

Catalysts	crystalline sizes/nm	crystallinity/%	Si/Al	S(m^2/g)			V (cm^3/g)		
				Total[a]	Micro[b]	External area[c]	Total[d]	Micro[e]	Meso[f]
HY	36.60	100.00	2.70	682	556	126	0.40	0.27	0.13
HY-DAl$_{0.11}$	33.50	58.39	5.49	816	552	264	0.46	0.22	0.24
HY-DAl$_{0.15}$	29.20	22.93	6.03	383	236	147	0.22	0.09	0.13
HY-DAl$_{0.15}$-DSi$_{NH4OH0.05}$	20.20	18.68	3.96	382	73	309	0.28	0.04	0.24
HY-DAl$_{0.11}$-DSi$_{NH4OH0.05}$	35.10	62.84	4.80	635	470	165	0.41	0.20	0.21
HY-DAl$_{0.11}$-DSi$_{NaOH0.05}$ (298 K)	34.40	55.20	4.68	710	478	232	0.47	0.21	0.26
HY-DAl$_{0.11}$-DSi$_{NaOH0.05}$	34.00	48.62	4.08	644	396	248	0.45	0.17	0.28
HY-DAl$_{0.11}$-DSi$_{NaOH0.10}$	32.80	40.98	3.25	386	193	193	0.40	0.13	0.27
HY-DAl$_{0.11}$-DSi$_{NaOH0.20}$	32.60	35.67	2.84	–	–	–	–	–	–

[a]BET surface area.
[b], [c], and [e] t-plot method.
[d]Volume adsorbed at $P/P_0 = 0.99$.
[f]$V_{Meso} = V_{Total} - V_{Micro}$.

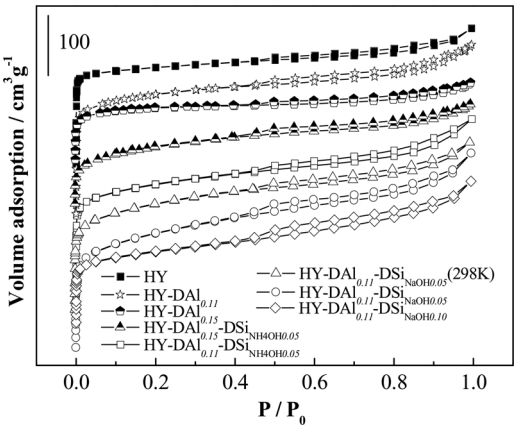

Fig. 2. N_2 sorption isotherms of as-treated zeolite catalysts.

mesopore size was unchanged with much weaker intensity of 0.055 $cm^3\,g^{-1}\,nm^{-1}$. After HY-DAl$_{0.15}$ treated with 0.05 M NH_4OH, the small mesoporous were re-emerged with 0.16 $cm^3\,g^{-1}\,nm^{-1}$ intensity. When HY-DAl$_{0.11}$ was further treated with different bases in the order of 0.05 M NH_4OH (298 K), 0.05 M NaOH (298 K), 0.05 M NaOH (338 K), and 0.10 M NaOH (338 K), the small mesopore size increased from 3.41 to 3.41, 3.42, 3.82, and 3.82 nm as well as the large mesopore size stayed at 17.53, 17.56, 17.40, and 9.60 nm; the small mesoporous intensity increased from 0.10 to 0.15, 0.18, 0.22, and 0.24 $cm^3\,g^{-1}\,nm^{-1}$ as well as the large mesopore peak intensity rose from 0.09 to 0.11, 0.12, 0.13, 0.15 $cm^3\,g^{-1}\,nm^{-1}$.

These results demonstrated that a certain concentration of H_4EDTA could contribute to the increase of microporous and large mesopore amount but reduce the pore sizes of microporous and small mesoporous because amorphous Al-rich debris, that decreased the pore size and further blocked the small mesoporous [28], were evidently generated after the excessive dealumination treatment. After dealumination by H_4EDTA solution, further desilication by bases mainly resulted in the increase of mesopore amount and small mesopore size but the reduction of micropore amount.

The analysis results of BET surface areas and pore volumes are displayed in Table 1. The external surface area, calculated by a t-plot method [41] and corresponded to the mesopore surface area [26], of HY, HY-DAl$_{0.11}$, HY-DAl$_{0.15}$, HY-DAl$_{0.15}$-DSi$_{NH4OH0.05}$, HY-DAl$_{0.11}$-DSi$_{NH4OH0.05}$, HY-DAl$_{0.11}$-DSi$_{NaOH0.05}$ (298 K), HY-DAl$_{0.11}$-DSi$_{NaOH0.05}$, and HY-DAl$_{0.11}$-DSi$_{NaOH0.10}$ were 126, 264, 147, 309, 165, 232, 248, and 193 m^2/g, respectively. Their mesopore volumes were 0.13, 0.24, 0.13, 0.24, 0.21, 0.26, 0.28, and 0.27 cm^3/g, respectively. The characterization results illustrated that the mesopore volume and specific

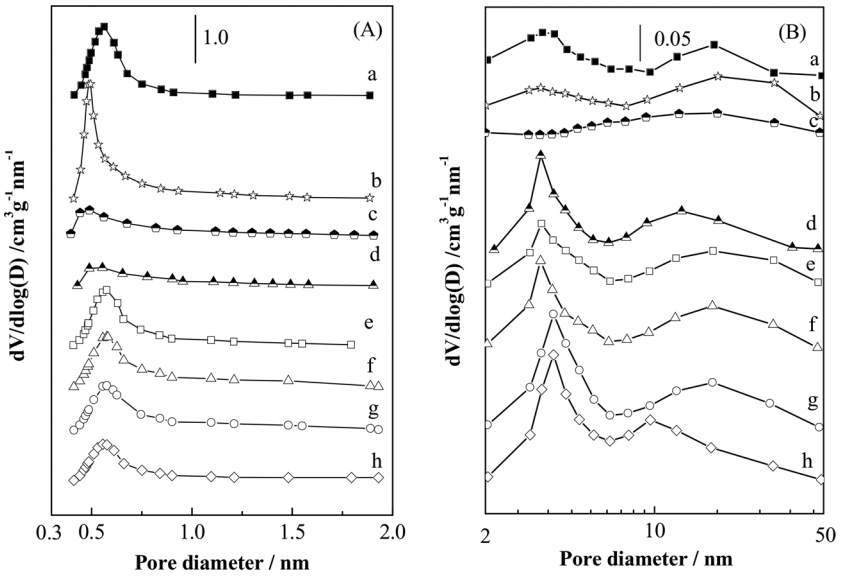

Fig. 3. The pore size distribution of as-treated catalysts (a) HY, (b) HY-DAl$_{0.11}$, (c) HY-DAl$_{0.15}$, (d) HY-DAl$_{0.15}$-DSi$_{NH4OH0.05}$, (e) HY-DAl$_{0.11}$-DSi$_{NH4OH0.05}$, (f) HY-DAl$_{0.11}$-DSi$_{NaOH0.05}$ (298 K), (g) HY-DAl$_{0.11}$-DSi$_{NaOH0.05}$, and (h) HY-DAl$_{0.11}$-DSi$_{NaOH0.10}$ in micropore region (A) and in mesopore region (B).

surface area of HY-DAl$_{0.11}$ were about twofold of HY. With increasing the H_4EDTA concentration to 0.15 M, the external surface area and mesopore volume, which were nearly the same as those of HY, significantly decreased. Further treated with bases, the volume of mesoporous and external surface area were two times higher than those of HY. Among these, the strong base of NaOH was more conducive to form mesoporous than that of weak base NH_4OH [36], but higher NaOH concentration led to the partial structure amorphization and resulted in the decrease of pore volume [37]. This phenomenon was also evidenced by the fact that the large mesopore size of HY-DAl$_{0.11}$-DSi$_{NaOH0.10}$ was significantly reduced, as displayed in Fig. 3(B). Under the heating condition, more mesoporous were introduced [28,36] as Si atoms were more easily extracted at higher temperature [42]. It could be seen from the characterization records that the generation of mesoporous was accompanied by the reduction of microporous, suggesting that the mesoporous were originated from the microporous during the acid or alkaline treatment as the extraction of framework atoms caused the collapsion of the micropore walls and resulted in the formation of mesoporous [26,43].

3.3. NH_3-TPD analysis of as-treated catalysts

The acidity of zeolite catalysts was measured by NH_3-TPD and compared in Fig. 4. All samples displayed two NH_3 desorption peaks at 370–550 K corresponded to the weak acid sites and at 550–850 K attributed to medium-strong acid sites [44–49]. The acidity content was calculated according to the desorbed amount of NH_3 and summarized in Table 2. The weak acid amount of HY, HY-DAl$_{0.11}$, HY-DAl$_{0.15}$, HY-DAl$_{0.15}$-DSi$_{NH4OH0.05}$, HY-DAl$_{0.11}$-DSi$_{NH4OH0.05}$, HY-DAl$_{0.11}$-DSi$_{NaOH0.05}$, and HY-DAl$_{0.11}$-DSi$_{NaOH0.10}$ were 1.684, 0.717, 0.315, 0.285, 0.781, 0.769, and 0.690 mmol g^{-1} as well as their medium-strong acid amount were 0.530, 0.205, 0.127, 0.092, 0.177, 0.166, and 0.068 mmol g^{-1}, respectively. As expected, the acid amount including the weak and medium-strong acid sites was significantly influenced by the variation of dealumination degree. The acid amount gradually decreased with the increased H_4EDTA concentration. For further desilication, the amount of both weak and medium-strong acids also decreased. Among these, the total acid amount of HY-DAl$_{0.11}$-DSi$_{NaOH0.05}$ was less than that of HY-DAl$_{0.11}$-DSi$_{NH4OH0.05}$.

After dealumination or desilication, the weak acid peak of all treated zeolites changed to lower temperature, suggesting that the strength of weak acid sites decreased. With the H_4EDTA concentration increasing from 0 to 0.15 M, the first TPD peak shifted from 468 to 435 K. Further treated with 0.05 M bases, the peak shifted to higher temperature range (443–452 K). Continually increasing the NaOH concentration to 0.10 M, the peak decreased to 440 K. When the parent HY was treated with 0.11 M H_4EDTA, the peak of medium-strong acid decreased to 618 K. With the H_4EDTA concentration increasing to 0.15 M, the medium-strong acid peak almost disappeared. Further desilication by 0.05 M NH_4OH or NaOH, the temperature increased to 634 or 644 K. With desilication by 0.1 M NaOH, the peak of medium-strong acid also disappeared. The above-mentioned phenomena illustrated that after dealumination or desilication, the strength of both weak acid and medium-strong acid decreased as compared with that of parent HY because the higher desorption temperature of NH_3 was attributed to the greater acid strength of as-used zeolite sites. For the only dealumination process, the acid strength gradually decreased with the increased H_4EDTA concentration and even the medium-strong acid site almost vanished when the H_4EDTA concentration increased to 0.15 M. For further desilication by using appropriate concentration bases (0.05 M NH_4OH or NaOH), the strength of both weak and medium-strong acids increased while the medium-strong acid site practically disappeared with the NaOH concentration increasing to 0.10 M.

Table 2
The acidity distribution of catalysts.

Catalysts	Weak acid amount/ mmol g^{-1} T_1/370–550 K	Strong acid amount/ mmol g^{-1} T_2/550–850 K	Total acid amount/ mmol g^{-1}
HY	1.684	0.530	2.214
HY-DAl$_{0.11}$	0.717	0.205	0.992
HY-DAl$_{0.15}$	0.315	0.127	0.442
HY-DAl$_{0.15}$-DSi$_{NH4OH0.05}$	0.285	0.092	0.385
HY-DAl$_{0.11}$-DSi$_{NH4OH0.05}$	0.781	0.177	0.958
HY-DAl$_{0.11}$-DSi$_{NaOH0.05}$	0.769	0.166	0.935
HY-DAl$_{0.11}$-DSi$_{NaOH0.10}$	0.690	0.068	0.758

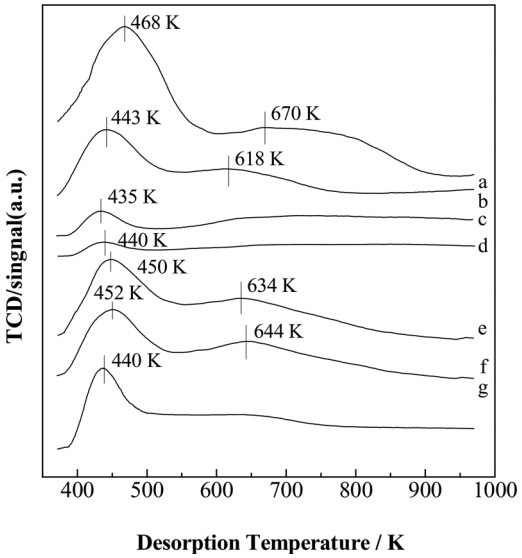

Fig. 4. NH_3-TPD curves of as-treated catalysts (a) HY, (b) HY-DAl$_{0.11}$, (c) HY-DAl$_{0.15}$, (d) HY-DAl$_{0.15}$-DSi$_{NH4OH0.05}$, (e) HY-DAl$_{0.11}$-DSi$_{NH4OH0.05}$, (f) HY-DAl$_{0.11}$-DSi$_{NaOH0.05}$, and (g) HY-DAl$_{0.11}$-DSi$_{NaOH0.10}$.

3.4. TG-DTA analysis of the as-used catalysts after reaction

The TG-DTA curves of as-used catalysts HY and HY-DAl$_{0.11}$-DSi$_{NaOH0.05}$ after 20 h reaction at 5.0 MPa and 393 K are displayed in Fig. 5(A) and (B). Both DTA profiles of HY and HY-DAl$_{0.11}$-DSi$_{NaOH0.05}$ exhibited one endothermic and three exothermic peaks. The endothermic peak was assigned to the desorption of physical adsorbed water [50]. The first exothermic peak was associated to the combustion of adsorbed impurities. The second exothermic peak was related to the burning of the soft coke [51] that was the organic intermediates such as methoxyacetyl or hemiacetal substance [15,18] formed during the reaction. The third exothermic peak was assigned to the combustion of heavy coke [52–54]. For HY after reaction, the combustion temperatures of soft and heavy coke were 685 and 1000 K, as well as the amount were 3.47% and 3.02%, respectively. For HY-DAl$_{0.11}$-DSi$_{NaOH0.05}$ after reaction, the burnt temperature (680 K) and amount (3.10%) of soft coke were nearly the same as those of HY. However, the weight loss (0.46%) of carbon deposition was only about 15.23% and much lower than that of HY, indicating that the coke formation was effectively suppressed in the mesoporous of HY-DAl$_{0.11}$-DSi$_{NaOH0.05}$ during the whole carbonylation process. We considered that the carbon deposition was closely related to the acid strength and mass-transfer efficiency of the as-treated catalysts. The weaker acid strength and mesopore structure contributed to the reduction of coke. As proved, the acid amount and acid strength of HY-DAl$_{0.11}$-DSi$_{NaOH0.05}$ were lower

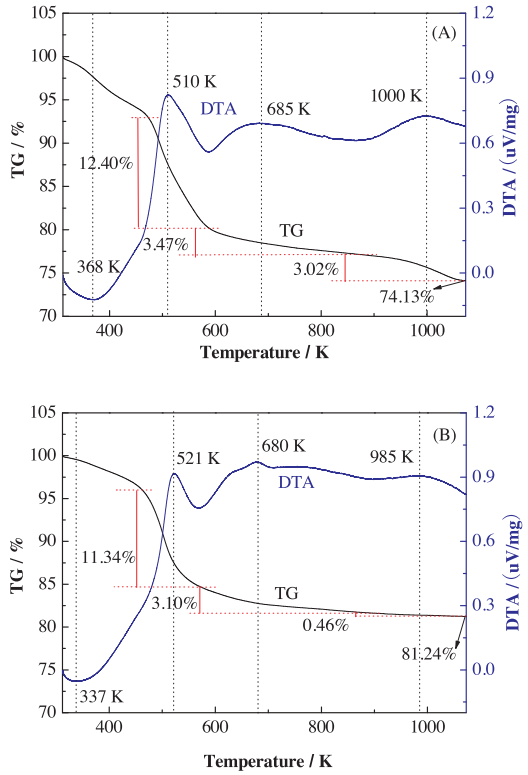

Fig. 5. TG-DTA curves of as-used catalysts (A) HY and (B) HY-DAl$_{0.11}$-DSi$_{NaOH0.05}$ after 20 h reaction.

than those of HY, as well as the external surface area and mesopore volume of HY-DAl$_{0.11}$-DSi$_{NaOH0.05}$ was much larger than those of HY, resulting in less carbon deposition formation.

3.5. Catalytic behaviors of hierarchical HY zeolites for DMM carbonylation

The vapor phase carbonylation of DMM was conducted at 5.0 MPa and 383 K using parent HY and different hierarchical HY zeolites. As displayed in Fig. 6, the DMM conversion of HY was very low and only about 50.41%. After dealumination or desilication pretreatment, the DMM conversion of HY-DAl$_{0.11}$, HY-DAl$_{0.15}$, HY-DAl$_{0.15}$-DSi$_{NH4OH0.05}$, HY-DAl$_{0.11}$-DSi$_{NH4OH0.05}$, HY-DAl$_{0.11}$-DSi$_{NaOH0.05}$ (298 K), HY-DAl$_{0.11}$-DSi$_{NaOH0.05}$, HY-DAl$_{0.11}$-DSi$_{NaOH0.10}$, and HY-DAl$_{0.11}$-DSi$_{NaOH0.20}$ significantly increased and was 99.56%, 80.68%, 71.83%, 92.21%, 95.44%, 90.91%, 64.22%, and 56%, respectively. Combined with the

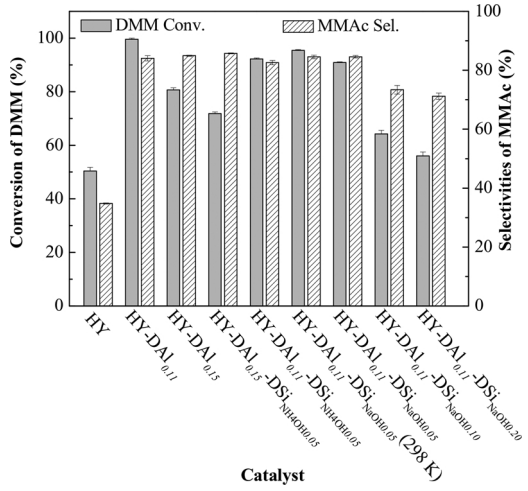

Fig. 6. The influence of different zeolite catalysts on DMM carbonylation.

NH_3-TPD characterization results in Table 2, the medium-strong acid amount (except for HY-DAl$_{0.11}$-DSi$_{NaOH0.20}$) was 0.205, 0.127, 0.092, 0.177, 0.166, and 0.068 mmol g^{-1}, respectively. It was concluded that the DMM conversion of the as-treated zeolites were strictly in accordance with the medium-strong acid amount. Greater amount of medium-strong acid sites resulted in higher DMM conversion. It was deduced that the lowest DMM conversion of parent HY was assigned to the mass-transfer control of products with large molecular weight although HY had the largest medium-strong acid amount.

The MMAc selectivity of reference HY was extremely low and only about 34.79%. After dealumination or desilication process, the MMAc selectivity of HY-DAl$_{0.11}$, HY-DAl$_{0.15}$, HY-DAl$_{0.15}$-DSi$_{NH4OH0.05}$, HY-DAl$_{0.11}$-DSi$_{NH4OH0.05}$, HY-DAl$_{0.11}$-DSi$_{NaOH0.05}$ (298 K), HY-DAl$_{0.11}$-DSi$_{NaOH0.05}$, HY-DAl$_{0.11}$-DSi$_{NaOH0.10}$, and HY-DAl$_{0.11}$-DSi$_{NaOH0.20}$ was obviously enhanced and about 84.04%, 84.93%, 85.74%, 82.57%, 84.55%, 84.57%, 73.36%, and 71.20%, respectively. According to the pore sizes distribution in Fig. 3(B), the MMAc selectivity of as-treated zeolites with large mesopore sizes centered at around 17.40–18.32 nm stayed nearly the same and was in the range from 82.57% to 85.74% while the large mesopore size of HY-DAl$_{0.11}$-DSi$_{NaOH0.10}$ shifted to 9.6 nm, leading to the lower MMAc selectivity (73.36%). For HY-DAl$_{0.11}$-DSi$_{NaOH0.10}$, the mesopore volume and external surface area clearly decreased as compared with those of HY-DAl$_{0.11}$-DSi$_{NaOH0.05}$ because of the partial collapsion of FAU structure caused by higher NaOH concentration pretreatment.

We considered that the diffusion and mass transfer efficiency of MMAc was limited in HY micropore channels and large molecular weight (104.1 g/mol). More importantly, a low mass transfer rate of MMAc could result in the deactivation of as-used catalyst because the heavy products remaining on the acid centers in the channels were beneficial for the formation of the carbon deposition, that readily covered the active sites, as proved by TG-DTA analysis in Fig. 5(A). Hence, the mesopore structure of as-treated HY (as shown in Fig. 3 and Table 1) with larger external surface area and mesopore volume significantly contributed to the mass transfer rate of MMAc, leading to the increased DMM conversion and MMAc selectivity.

3.6. The influence of reaction temperatures on DMM carbonylation

The effect of reaction temperatures from 363 to 433 K on DMM carbonylation with 1 g HY and HY-DAl$_{0.11}$-DSi$_{NaOH0.05}$ are exhibited in Fig. 7(A) and (B). For HY-DAl$_{0.11}$-DSi$_{NaOH0.05}$ in Fig. 7(B), it could be seen that the conversion of DMM gradually increased from 22.54% to 99.59% with the temperature increasing from 363 to 433 K. With gradually rising the temperature (363–373 K), the selectivity of dimethyl ether (DME) decreased from 16.96% to 8.16%; the selectivity of methyl formate (MF) sharply decreased from 34.25% to 2.37%; and the selectivity of methanol (MeOH) significantly decreased from 43.27% to 4.45%. Meanwhile, the selectivity of MMAc increased and reached a maximum of 85.02% at 373 K. When the reaction temperature further increased from 383 to 433 K, the selectivity of DME and MF gradually increased from 9.89% to 34.46% and from 2.73% to 5.34%. The selectivity of MeOH slowly decreased from 2.81% to 1.84%. The selectivity of MMAc gradually decreased from 84.57% to 56.59%. The Methyl glycolate (MG) was produced and the selectivity continuously increased to 1.77%.

According to the literatures and former work [14–18], MMAc was formed from the direct carbonylation of DMM; DME and MF was generated from the disproportionation of DMM; MeOH was produced from the decomposition of MF or from the hydrolysis of DMM [14–16]; dissociative formaldehyde was also formed form the hydrolysis of DMM [14–16]; MG was created from the esterification of glycolic acid (GA) with MeOH [15]; and GA was produced from carbonylation of formaldehyde [55]. As stated, the MMAc selectivity was mainly influenced by two competitive reactions: DMM carbonylation and DMM disproportionation. At 363 K, the relative rate of disproportionation was

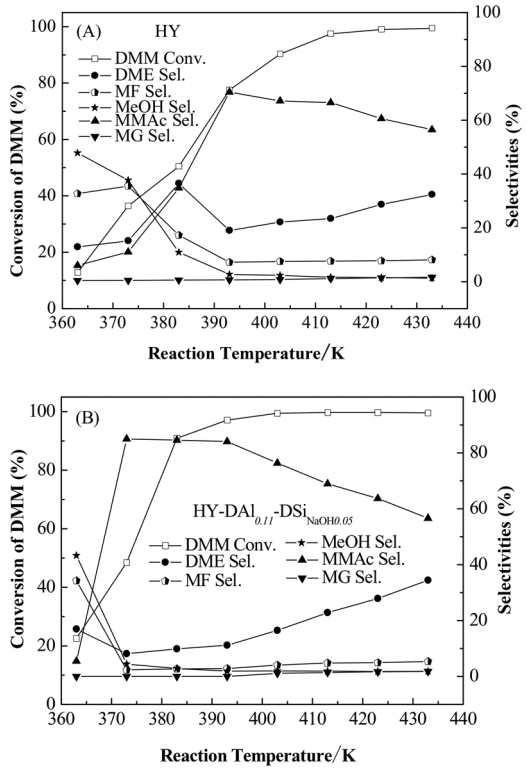

Fig. 7. The influence of reaction temperatures on DMM carbonylation using (A) HY and (B) HY-DAl$_{0.11}$-DSi$_{NaOH0.05}$.

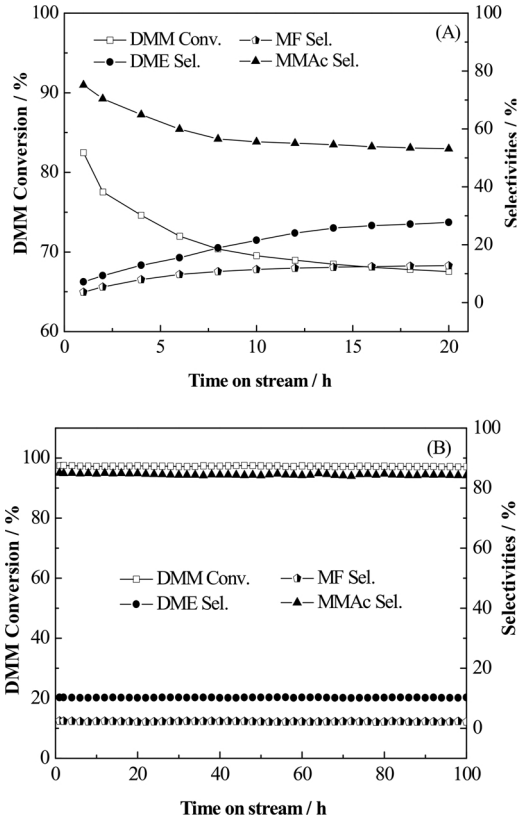

Fig. 8. The carbonylation stability of (A) HY for 20 h and (B) HY-DAl$_{0.11}$-DSi$_{NaOH0.05}$ for 100 h.

much higher than that of DMM carbonylation. Therefore, the selectivity of DME was higher than that of MMAc. When the temperature increased to 373 K, both carbonylation and disproportionation reactions rates were promoted, but the carbonylation rate was higher than that of DMM disproportionation. Hence, the MMAc selectivity was higher. With further increasing the reaction temperature, the increase of disproportionation rate was higher than that of carbonylation, leading to the gradually decreased MMAc selectivity and the continually increased DME selectivity. MG was produced from the cabonylation of formaldehyde [15] and the cabonylation efficiency was gradually promoted with the temperature increasing to 433 K.

The DMM conversion and MMAc selectivity variation trends of HY with temperature changing from 363 to 433 K in Fig. 7(A) were nearly the same as those of HY-DAl$_{0.11}$-DSi$_{NaOH0.05}$ in Fig. 7(B). However, the highest MMAc selectivity (70.41%) appeared at 393 K, that was about 14.61% lower and 20 K higher than those of HY-Dl$_{0.11}$-DSi$_{NaOH0.05}$ after dealumination and desilication operation, illustrating that the mass transfer efficiency of as-treated zeolite catalysts was significantly enhanced. The effect of reaction temperatures for the other treated catalysts are displayed in Fig. S1 and exhibited the similar rules.

3.7. Catalytic stability of HY and HY-DAl$_{0.11}$-DSi$_{NaOH0.05}$

The carbonylation stability of HY and HY-DAl$_{0.11}$-DSi$_{NaOH0.05}$ was carried out at 393 K and 5.0 MPa. The DMM conversion as well as DME, MF, and MMAc selectivity of HY with time on stream for 20 h are displayed in Fig. 8(A). For the initial 8 h, the DMM conversion dropped rapidly from 82.46% to 70.38% and the MMAc selectivity significantly decreased from 75.19% to 56.53%. Meanwhile, the DME selectivity obviously increased from 7.16% to 18.89% and the MF selectivity raised from 3.64% to 10.72%. After 10 h, the HY catalyst slowly lost its activity from 69.52% to 67.55% until 20 h with MMAc selectivity gradually declining from 55.55% to 53.12%. The catalytic performance of HY-DAl$_{0.11}$-DSi$_{NaOH0.05}$ is shown in Fig. 8(B). It was clearly that the DMM conversion (about 97%) and products selectivity (MMAc: 84%) kept unchanged during 100 h reaction, indicating that the activity of as-treated HY-DAl$_{0.11}$-DSi$_{NaOH0.05}$ was very stable. It was inferred that the excellent activity and stability of HY-DAl$_{0.11}$-DSi$_{NaOH0.05}$ were attributed to its outstanding mass transfer ability in mesopore structure. The only deactivation reason of as-used zeolite catalysts in this reaction system was assigned to the carbon deposition because the reactant and products were neutral and could not lead to the dealumination or desilication. The TG-DTA results also proved that HY-DAl$_{0.11}$-DSi$_{NaOH0.05}$ was highly resistant to coke formation. Therefore, as-treated HY-DAl$_{0.11}$-DSi$_{NaOH0.05}$ with larger external surface area and mesopore volume exhibited efficient mass transfer rate, resulting in excellent stability even through 100 h reaction.

4. Conclusions

In summary, a series of hierarchical HY zeolite had been successfully prepared using a method of post-synthetic treatments including acid (H_4EDTA) and alkali (NaOH or NH_4OH) treatments. According to the nitrogen adsorption-desorption analysis, the mesopore structure was definitely formed with the pore diameter at about 3.5 and 17.5 nm. The external surface area and mesopore volume of treated HY zeolites significantly increased by a certain concentration of H_4EDTA and bases pretreatment, but the XRD analysis suggested that the relative crystallinity and crystalline sizes simultaneously decreased. The XRF analysis disclosed that the Si/Al ratios of as-treated HY zeolites were higher than that of parent HY zeolite while the NH_3-TPD analysis indicated that the acid amount and strength gradually decreased with the increased H_4EDTA or bases concentration. The DMM conversion were strictly related to the medium-strong acid amount and greater amount of medium-strong acid sites resulted in higher DMM conversion. As-treated HY zeolites exhibited much higher DMM conversion and MMAc selectivity because the larger external surface area and mesopore volume contributed to greater mass transfer efficiency, leading to much

less carbon deposition, which was supported by the TG-DTA analysis that the coke formation was effectively suppressed. HY-$DAl_{0.11}$-$DSi_{NaOH0.05}$ exhibited excellent activity (DMM cov. = 97%, MMAc sel. = 84%) and stability at 393 K and 5.0 MPa for 100 h reaction process. It was anticipated this direct carbonylation of DMM to MMAc catalyzed by highly active, selective, and stable hierarchical HY zeolites was promising for industrial applications.

Acknowledgements

This work was supported by the National Natural Science Foundation of China (21303106); Natural Science Foundation of Liaoning Province (2015020243); The first class General Financial Grant from the China Postdoctoral Science Foundation (2014M560224); A Special Financial Grant from the China Postdoctoral Science Foundation (2015T80275).

Appendix A. Supplementary data

Supplementary data associated with this article can be found, in the online version, at https://doi.org/10.1016/j.cattod.2018.02.004.

References

[1] K.P. de Jong, J. Zečević, H. Friedrich, P.E. de Jongh, M. Bulut, S. van Donk, R. Kenmogne, A. Finiels, V. Hulea, F. Fajula, Angew. Chem. Int. Ed. 49 (2010) 10074–10078.
[2] I.I. Ivanova, A.S. Kuznetsov, V.V. Yuschenko, E.E. Knyazeva, Pure Appl. Chem. 76 (2004) 1647–1657.
[3] C. Xing, J. Sun, G.H. Yang, W.Z. Shen, L. Tan, P.F. Zhu, Q.H. Wei, J. Li, M. Kyodo, R.Q. Yang, Y. Yoneyama, N. Tsubaki, Fuel Process. Technol. 136 (2015) 68–72.
[4] L. Gueudré, M. Milina, S. Mitchell, J. Pérez-Ramírez, Adv. Funct. Mater. 24 (2014) 209–219.
[5] X.F. Li, R. Prins, J.A. van Bokhoven, J. Catal. 262 (2009) 257–265.
[6] A.N.C. van Laak, S.L. Sagala, J. Zečević, H. Friedrich, P.E. de Jongh, K.P. de Jong, J. Catal. 276 (2010) 170–180.
[7] Y.Y. Sun, R. Prins, Appl. Catal. A-Gen. 336 (2008) 11–16.
[8] K. Cheng, J.C. Kang, S.W. Huang, Z.Y. You, Q.H. Zhang, J.S. Ding, W.Q. Hua, Y.C. Lou, W.P. Deng, Y. Wang, ACS Catal. 2 (2012) 441–449.
[9] M.S. Holm, E. Taarning, K. Egeblad, C.H. Christensen, Catal. Today 168 (2011) 3–16.
[10] S.-H. Kim, D.B. Chun, S.-D. Yoon, H.-S. Byun, J. Chem. Eng. Data 61 (2016) 1101–1108.
[11] Q.H. Li, C.H. Huang, T.W. Xu, J. Membr. Sci. 339 (2009) 28–32.
[12] D.H. He, W.G. Huang, J.Y. Liu, Q.M. Zhu, J. Mol. Catal. A-Chem. 145 (1999) 335–338.
[13] K.B. Wang, J. Yao, Y. Wang, G.Y. Wang, J. Nat. Gas Chem. 16 (2007) 286–292.
[14] F.E. Celik, T.-J. Kim, A.T. Bell, Angew. Chem. Int. Ed. 121 (2009) 4907–4909.
[15] L. Shi, J. Yao, W.L. Zhu, Z.M. Liu, J. CIESC 68 (2017) 3739–3746.
[16] F.E. Celik, T.-J. Kim, A.T. Bell, J. Catal. 270 (2010) 185–195.
[17] F.E. Celik, T.-J. Kim, A.N. Mlinar, A.T. Bell, J. Catal. 274 (2010) 150–162.
[18] V. Shapovalov, A.T. Bell, J. Phys. Chem. C 114 (2010) 17753–17760.
[19] D. Verboekend, N. Nuttens, R. Locus, J. Van Aelst, P. Verolme, J.C. Groen, J. Perez-Ramirez, B.F. Sels, Chem. Soc. Rev. 45 (2016) 3305–3566.
[20] R. Chal, T. Cacciaguerra, S. van Donk, C. Gerardin, Chem. Commun. 46 (2010) 7840–7842.
[21] Z. Wang, H.H. Liu, Q.T. Meng, J.S. Jin, C.Y. Xu, X.T. Mi, X.H. Gao, H.T. Liu, RSC Adv. 7 (2017) 9605–9609.
[22] B. Sulikowski, J. Phys. Chem. 97 (1993) 1420–1425.
[23] D. Verboekend, T.C. Keller, S. Mitchell, J. Pérez-Ramírez, Adv. Funct. Mater. 23 (2013) 1923–1934.
[24] C.S. Triantafillidis, A.G. Vlessidis, N.P. Evmiridis, Ind. Eng. Chem. Res. 39 (2000) 307–319.
[25] Z.X. Qin, B.J. Shen, X.H. Gao, F. Lin, B.J. Wang, C.M. Xu, J. Catal. 278 (2011) 266–275.
[26] D. Verboekend, J. Pérez-Ramírez, Catal. Sci. Technol. 1 (2011) 879–890.
[27] H.X. Tao, C.L. Li, J.W. Ren, Y.Q. Wang, G.Z. Lu, J. Solid State Chem. 184 (2011) 1820–1827.
[28] D. Verboekend, G. Vilé, J. Pérez-Ramírez, Adv. Funct. Mater. 22 (2012) 916–928.
[29] Y.S. Tao, H. Kanoh, L. Abrams, K. Kaneko, Chem. Rev. 106 (2006) 896–910.
[30] J. Van Aelst, D. Verboekend, A. Philippaerts, N. Nuttens, M. Kurttepeli, E. Gobechiya, M. Haouas, S.P. Sree, J.F.M. Denayer, J.A. Martens, C.E.A. Kirschhock, F. Taulelle, S. Bals, G.V. Baron, P.A. Jacobs, B.F. Sels, Adv. Funct. Mater. 25 (2015) 7130–7144.
[31] W.Q. Jiao, W.H. Fu, X.M. Liang, Y.M. Wang, M.-Y. He, RSC Adv. 4 (2014) 58596–58607.
[32] Y. Goa, H. Yoshitake, P. Wu, T. Tatsumi, Microporous Mesoporous Mater. 70 (2004) 93–101.
[33] M. Sprynskyy, R. Golembiewski, G. Trykowski, B. Buszewski, J. Phys. Chem. Solids 71 (2010) 1269–1277.
[34] D.P. Serrano, J.M. Escola, P. Pizarro, Chem. Soc. Rev. 42 (2013) 4004–4035.
[35] A. Čimek, B. Subotić, I. Šmit, A. Tonejc, R. Aiello, F. Crea, A. Nastro, Microporous Mesoporous Mater. 8 (1997) 159-169.
[36] J. Perez-Ramirez, S. Abello, L.A. Villaescusa, A. Bonilla, Angew. Chem. Int. Ed. 120 (2008) 8031–8035.
[37] T. Suzuki, T. Okuhara, Microporous Mesoporous Mater. 43 (2001) 83–89.
[38] J. Van Aelst, M. Haouas, E. Gobechiya, K. Houthoofd, A. Philippaerts, S.P. Sree, C.E.A. Kirschhock, P.A. Jacobs, J.A. Martens, B.F. Sels, F. Taulelle, J. Phys. Chem. C 118 (2014) 22573–22582.
[39] C. Xing, G.H. Yang, M.B. Wu, R.Q. Yang, L. Tan, P.F. Zhu, Q.H. Wei, J. Li, J.W. Mao, Y. Yoneyama, N. Tsubaki, Fuel 148 (2015) 48–57.
[40] A.H. Janssen, A.J. Koster, K.P. de Jong, Angew. Chem. Int. Ed. 40 (2001) 1102–1104.
[41] R.W. Cranston, F.A. Inkley, Adv. Catal. 9 (1957) 143–154.
[42] J.C. Groen, J.C. Jansen, J.A. Moulijn, J. Pérez-Ramírez, J. Phys. Chem. B 108 (2004) 13062–13065.
[43] J. Pérez-Ramírez, D. Verboekend, A. Bonilla, S. Abelló, Adv. Funct. Mater. 19 (2009) 3972–3979.
[44] J.J. Zheng, Y.M. Yi, W.L. Wang, K. Guo, J.H. Ma, R.F. Li, Microporous Mesoporous Mater. 171 (2013) 44–52.
[45] G.H. Yang, N. Tsubaki, J. Shamoto, Y. Yoneyama, Y. Zhang, J. Am. Chem. Soc. 132 (2010) 8129–8136.
[46] D.F. Jin, B. Zhu, Z.Y. Hou, J.H. Fei, H. Lou, X.M. Zheng, Fuel 86 (2007) 2707–2713.
[47] F. Yaripour, F. Baghaei, I. Schmidt, J. Perregaard, Catal. Commun. 6 (2005) 147–152.
[48] F. Arena, R. Dario, A. Parmaliana, Appl. Catal. A 170 (1998) 127–137.
[49] N. Taufiqurrahmi, A.R. Mohamed, S. Bhatia, J. Nanopart. Res. 13 (2011) 3177–3189.
[50] L. Shi, C.Y. Zeng, Q.H. Lin, P. Lu, W.Q. Niu, N. Tsubaki, Catal. Today 228 (2014) 206–211.
[51] H. Zhou, W.L. Zhu, L. Shi, H.C. Liu, S.P. Liu, S.T. Xu, Y.M. Ni, Y. Liu, L.N. Li, Z.M. Liu, Catal. Sci. Technol. 5 (2015) 1961–1968.
[52] M.A. Camblor, A. Corma, S. Valencia, Microporous Mesoporous Mater. 25 (1998) 59–74.
[53] M. Guisnet, P. Magnoux, Appl. Catal. A-Gen. 212 (2001) 83–96.
[54] L. Palumbo, F. Bonino, P. Beato, M. Bjørgen, A. Zecchina, S. Bordiga, J. Phys. Chem. C 112 (2008) 9710–9716.
[55] S.Y. Lee, J.H. Kim, J.S. Lee, Y.G. Kim, Ind. Eng. Chem. Res. 32 (1993) 253–259.